Ionospheric Mapping with the GPS/MET

George Hajj and Larry Romans
Jet Propulsion Laboratory, California Institute of Technology

Proceedings of the Institute of Navigation 52nd Annual Meeting, Cambridge, Massachusetts, June 19-21, 1996.

BIOGRAPHIES

Dr. George Hajj is a Member of the Technical Staff at the Jet Propulsion Laboratory in the Tracking Systems and Applications Section. He received his Ph.D. in physics from Rice University in 1988. His research experience and interests are in the areas of radio propagation and scattering, tomographic imaging, and GPS radio occultation techniques and applications.

Dr. Larry Romans received his Ph.D. in theoretical physics from Caltech in 1985. He is currently a Member of the Technical Staff in the Space Geodesy and Geodynamics Group at JPL, where his work has focused on geodetic applications of GPS.

ABSTRACT

The GPS/MET experiment, which placed a GPS receiver in a low-Earth orbit tracking the GPS in an occultation geometry, has collected thousands of occultations since its launch in April of 1995. Each occultation can be inverted to give an electron density profile in the ionosphere, temperature and pressure profiles in the lower mesosphere, stratosphere and upper troposphere, and water vapor density profiles in the lower troposphere.

This paper gives a summary of the ionospheric effects on the GPS/MET signal and examines some of the retrieved electron density profiles. We examine the bending induced by the ionosphere on the occulting signal and the resulting separation of the two GPS links corresponding to the L1 and L2 phase signals. We also examine the amplitude scintillation caused by sharp layers at the bottom of the ionosphere. We briefly describes the Abel inversion method for obtaining the index of refraction and show several examples of electron density profiles and comparisons to profiles derived from the Parametrized Ionospheric Model (PIM) and to incoherent scatter radar measurements.

1-INTRODUCTION

Since its launch in April 1995, the GPS/MET experiment, which placed a GPS receiver in a low-Earth orbit tracking the GPS in an occultation geometry, has collected thousands of occultations. A sizable fraction of these occultations have been analyzed to assess the benefits of the GPS radio occultation technique in the areas of ionospheric and neutral atmospheric remote sensing and to recommend changes to future generation flight receivers.

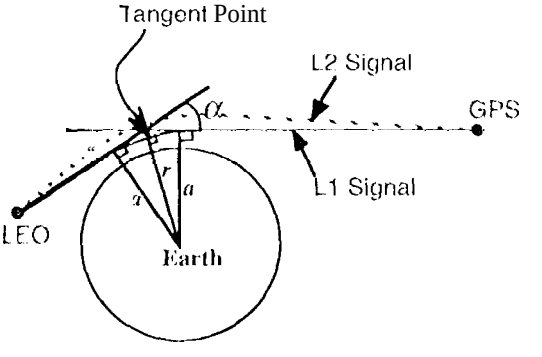

Fig. 1: Occultation geometry defining a, r, a and the tangent point and showing the separation of the L1 and L2 signals due to the dispersive ionosphere.

The basic concept of the GPS radio occultation technique is a simple one. When the L1 and L2 GPS signals propagate through the Earth's atmosphere as the GPS satellite is setting or rising with respect to a receiver in low-Earth orbit [Fig. 1] the signals' phase and amplitude are affected in ways that are characteristic of the index of refraction of the propagating media. When the entire signal is in the ionosphere, (i.e. the tangent point is above ~60 km) a single frequency is sufficient to obtain a vertical profile of the index of refraction in the ionosphere from which electron density can be derived. To obtain such a profile, certain assumptions regarding the

horizontal variability of the index of refraction ought [o be made. In the absence of any other information, a first-order solution can be obtained by assuming spherical symmetry. Then, the inversion method relies on estimating the bending of the occulting signal which is derived from isolating the excess Doppler shift induced by the atmosphere. The index of Infraction is then derived from bending via an Abel integral transform. This method has been applied extensively in NASA's planetary occultation experiments [see e.g. Fjeldbo, 1971 anti Tyler, i 987]. and was inherited from the area of geological mapping of the Earth's interior. The same technique is applied when the signal passes through the neutral atmosphere (tangent point below -60 km). The only difference is that in this situation two frequencies are needed to calibrate for the overlaying ionosphere and isolate the neutral atmospheric bending. Once the neutral atmospheric refractivity (which is proportional to density in the absence of water vapor) is obtained, the neutral density can be integrated vertically to obtain the pressure at a give height, The ideal gas law can then be used to derive temperature as a function of height. In the presence 01 significant amounts 01 water vapor (such as in (he lower troposphere), independent temperature data can be used in order [0 derive water vapor density.

The details of how the GPS/MET signal is calibrated in order to isolate the atmospheric effects on the occulting signals are given elsewhere [Hajj et al., 199 S]. Some early results of temperature retrievals anti comparisons to atmospheric models and radio osondes demonstrated that GPS/MET temperature profiles are accurate to better than 2K between -5-30 altitudes [Kursinski et al., 1996a; Ware et al., 1996]. Theoretical estimates of temperature accuracy achievable with the GPS occultation technique are at the sub-Kelvin level below 40 km down to heights where specific humidity is negligible [Kursinski et al., i 996 b]. In the lower-troposphere, the GPS occultation data can be used to derive water vapor by constraining the temperature based on a numerical weather model. The accuracy obtained this way is between 5-50% depending on season, latitude and height which cie.firm the abundance of water vapor [Kursinski et al, 1995]. Another variable which is very useful to meteorological and climatological models is the geopotential height for a given pressure level. Geopotential heights derived from GPS/MET are demonstrated to be accurate to better than *20* meters [Leroy 1996].

In this paper we examine some aspects of the radio occultation signal as it propogates through the ionosphere, In section ? we will examine the bending of the GPS phase signal and the separation of the L1 anti L2 links in the ionosphere. In section 3 we will study the. coverage of the GPS/MET anti examine some retrieved electron density profiles. in this section we will also examine the amplitude of the. L1 and L2 signals and deduce some information about sharp layers at (tie bottom of the ionosphere..

2- BENDING AN]) SIGNAL SEPARATION IN THE IONOSPHERE

In the ionosphere, the index of refraction for the phase is give by the Appleton-Hartree formula which can be expended in powers of inverse frequency to yield

$$n = 1 - 40.3 \times \frac{n_e}{f^2} \qquad (1)$$

where n is the index of refraction, n_e is the electron density in m^{-3} and f is the operating frequency in Hz. Based on Snell's law, the bending of the signal locally is in the direction of the refractivity gradient. In a general and approximate sense, the gradient of refractivity in the ionosphere is pointing upward above the F2 and downward below the same peak. Therefore, the GPS signals will generally bend upward anti downward above anti below the F2 peak respectively. Examining the bending of the GPS L1 signal for 6 I GPS/MET occultations that take place on May 4, i 99S, we observe the following features [Fig. 2]

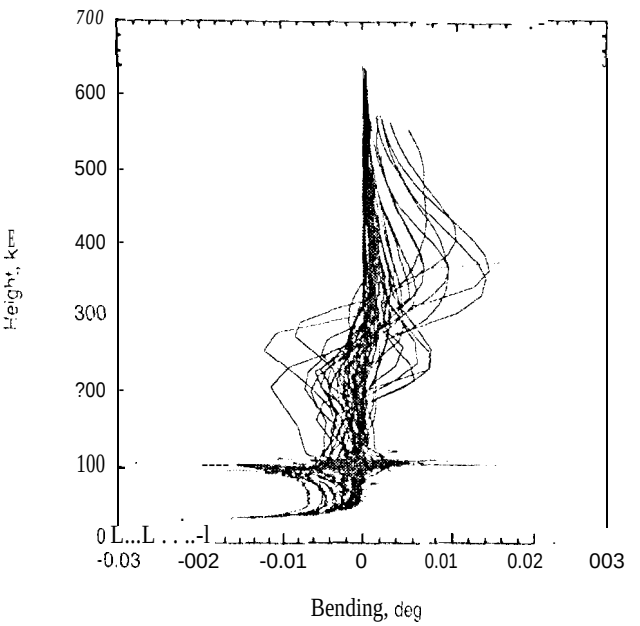

Fig. 2: Bending induced by the ionosphere on L1 signal for 61 globally distributed occultations on May 4, 1995. Negative bending is defined to be toward the Earth's center.

1-The bending varies about two orders of magnitude between 0,0001-0.01 degrees (cannot be seen from Fig. 2) depending on time-of-day and geographical location of the occultation consistent with variations of electron density profiles with the same variables. Since 1995 falls near a solar-minimum condition, the largest bending of figure 2 can be an order of magnitude smaller than the corresponding solar-maximum condition.

2-The highest peak in bending which is associated with the F2 peak varies in height between ~250-400 km which

is consistent with ionospheric profiles at different latitudes and local times.

3-With negative bending defined to be toward the earth, the signal bends away from (toward) the Earth above (below) well defined peaks in the ionosphere such as the I: I , F2 and the E peaks. Since the bending of the signal depends on the gradient Of the refractivity (which is vertical to first order), one expects to see a change of sign in the bending of the tangent point sample through a peak

4-The largest absolute bending for this particular day is ~0.03 degrees which corresponds to the signal just descending below the I ~-layer. The fact that the bending induced by the E-layer is larger than that of the F2 is due to the very short scale of the E-layer which makes the refractivity gradient largest there.

5-]'here is very sharp variation of bending which is associated with the Ii-1ayer,

6-The tails at the bottom end of all these curves coincide and starts to grow in magnitude due to the neutral atmospheric bending which starts to dominate at about 50 km altitude.

The most striking feature of these data is how sharp the signature is around the E- (or sporadic E-) layer, 1:ven though determination of the magnitude of the E-peak electron density might be obscured due to the overlaying layers (inversion of bending to obtain electron density will be discussed in the next section) the height of sharp E-layers can be determined very accurately. The bending derived from the time. derivative of phase provides one piece of information on the location of sharp layers in the ionosphere. The other piece of infor mation can be obtained from examination of the amplitude of the received phase which will be discussed in the next section.

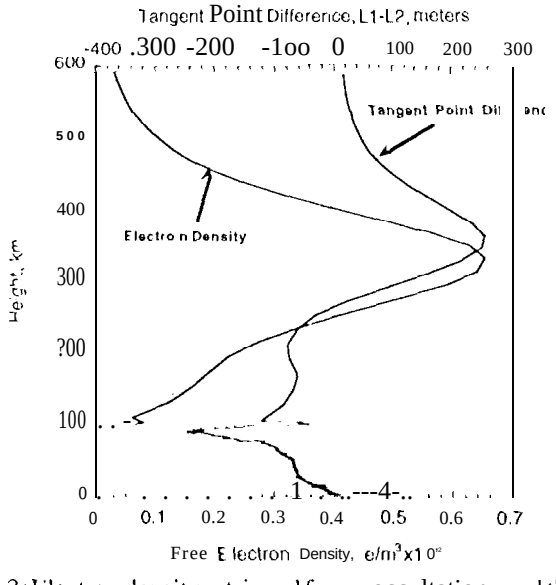

Fig. 3: Electron density retrieved from occultation and the corresponding amount of I,1 anti I.2 signal vertical separation

Bending for I.2 signal is a factor of 1 .65 (= square of the ratio of I, 1to 1,2 frequencies) larger (see Eq. (1)). This dispersive nature of the ionosphere causes the I .1 and I.2 signals to travel two slightly different paths and therefore sample different regions (see Fig. 1). This causes the tangent points of' the two links to be at different heights in the atmosphere at a specific time. Assuming spherical symmetry of electron density anti performing the Abel transform, the electron density profile and the height of the tangent point at a particular instant during the occultation can be solved for. Fig. 3 shows an example of an electron density retrieval obtained from GPS/MET for an occultation taking place near -6N latitude and 228E longitude around 20:04 UT of May 4, 1995. The corresponding local time is 1 I :01. Also shown on the figure is the separation between the 1. I anti I.2 tangent points as a function of altitude. In the neighborhood of the F2 peak, the relative position of the two signals change due to changing direction of bending. Above. the F2 peak, since the bending is generally up ward, the I.2 tangent point will always be lower that the 1,1, The situation reverses when the signal tangent point is below the F2 peak. For this particular profile, the maximum separation is of order 300 meters and it scales linearly with the amount of bending a signal experiences. Therefore, one can expect separations that are two orders of magnitude smaller (as seen with the bending) or onc order of magnitude larger during solar- max day-time. There is one positive and one negative implication to this separation. The positive implication is that the separation Of the two signals can bc used to deduce some in formation on the horizontal variation of the ionosphere. This is a topic which will be discussed under a sepal-ate paper. The negative implication is that in the neutral atmosphere, where the two signals are needed to calibrate for the ionosphere, a bigger ionospheric residual will remain in the "neutral atmospheric" bending when the separation of the two signal is large. in fact, unless a higher-order correction is made to the signal, the ionosphere can be the biggest limiting error source at altitudes above --40 km during solar-max day-time conditions [Kursinski et al., 1996b].

3. OCCULTATION COVERAGE AN]) ELECTRON D E NSITY PROFILING

A single antenna in a low-Earth orbit (LEO) tracking GPS with a 360" field-of-view will observe about 500" globally distributed occultations per day. Due to a narrower field-of-view of the GPS/MET antenna (± 30") and memory limitations on board the satellite, only 100-200" occultations per day are collected from the GPS/MET. A representative coverage of the occultations for one. day is shown in sun-fixed coordinates in Fig. 4, where each line corresponds to one occultation intersecting the ionosphere between 100-400 km altitude.

Because the coverage is shown as a function of sun-fixed longitude (0 sun-fixed longitude corresponds to noon local

time), and the fact that the occultations are scattered around the LEO orbit, the occultations arc concentrated around the ground track of the GPS/MET satellite. Al mid- and low-latitude the LEO samples the ionosphere at abo ut the same latitude. and local time for every LEO revolution. This local time will precess slowly with [he precession of the LEO orbit. For GPS/MET, it takes I 10 days for a lull prt'cession of' the satellite; therefore, it takes half of this period to sample the Earth at all local times for mid- and low-latitude. On the other hand, at high latitude, the same 12 hour period is sampled for a given hemisphere (e.g. in Fig. 4 the northern hemisphere is always sampled between noon and midnight local time whereas the souther II hemisphere i s sampled between midnight and noon local time). It takes half of the precession period to reverse the sampling geometry.

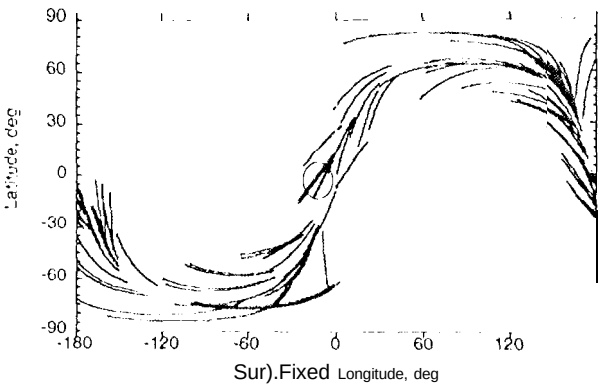

Fig. 4: (i} 'S/Ml II' coverage in sun-fixed coordinates in 24 hours, May 4, 1995.

The width of the spread of occultations around the LEO track is determined by the width of the field-of-view of the receiving antenna and the distance to the limb. For a 730 km altitude satellite (such as GPS/MET) the limb is about 3000 km away from the satellite. This implies that the tangent point of an occultation falls within a 3000 km radius from the satellite trajectory during that occultation; therefore, setting an upper limit on the width of the spread o f occultations around t h e LEO track t o be ~+ 27 equatorial degrees.

The reoccurrence of occultatio ns at nearby local times and latitudes is illustrated by strewing, the retrievals of four equatorial occultations appearing at consecutive orbital r e v o l u t i o n s each taking place near noon local time. (These four occultations cross the circle in the middle of Fig. 4.) The electron density retrievals (using the Abel transform) are shown in Fig. 5 which indicates the

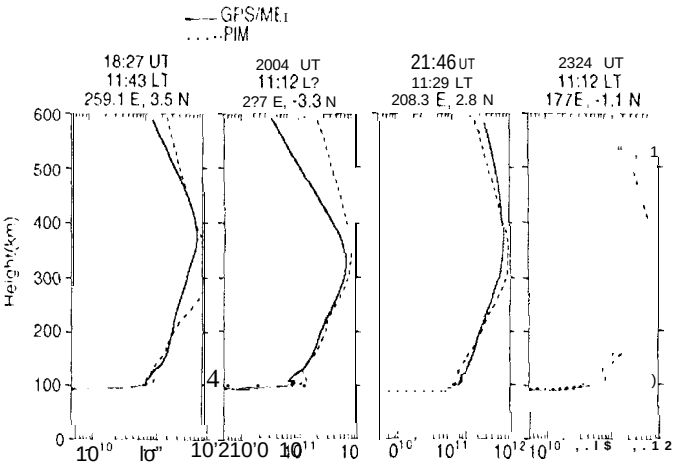

Fig. 5: Examples of electron density profiles (e/m^3) obtained from GPS/MET and PIM for equatorial latitude at abo ut the same local time.

For comparisons, profiles obtained from the Ionospheric Parameter ized Model (PIM) derived with input parameters suitable for the same day are also shown, Some of the main features to observe are: (1) the ability to observe the E-, F1- and F2-layers that are characteristics of mid- anti low-latitude day-time ionosphere, (2) The ability to observe the evolution of the ionosphere at the same local time and latitude every ~100 minutes (which is equal to the GPS/MET orbital period). Changes with time also reflect changes of magnetic dip latitude due to the rotation of the Earth. (3) Except for the far-left profile, the 1'IM reprod uces F2 peak densities and heights t h a t are i n reasonable agreement with the GPS/MET retrieval. (4) Compar isons with the PIM is generally better below the

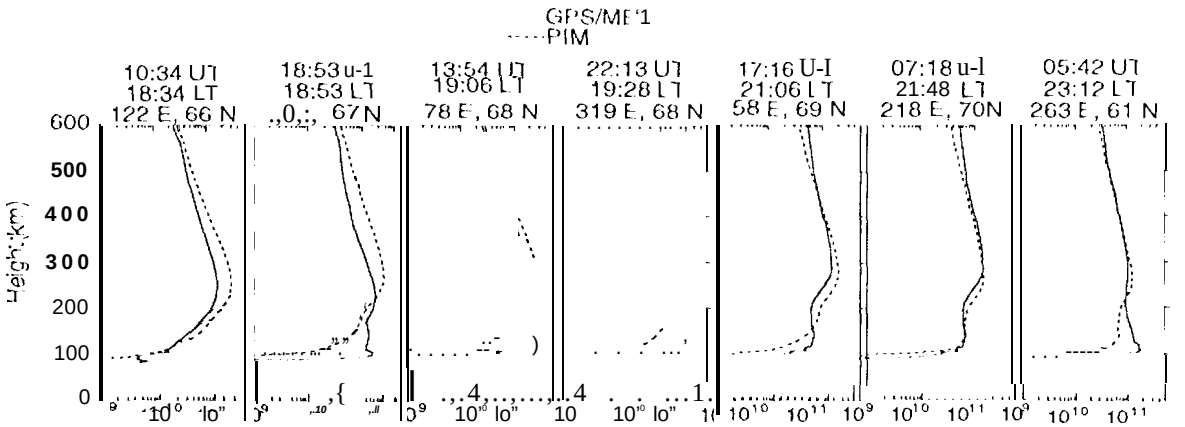

Fig. 6 Examples of high latitude electron density profiles obtained from GPS/MET and PIM

F2-peak than at the top-side. (5) The ability of both the model and the retrievals to reproduce [he sharp bottom of the ionosphere. Other examples of GPS/MET retrieved profiles are shown for high latitude between dusk and midnight local time. We note the much lower hmF2-peak height, the almost disappearance of the F1-peak, the recession of the F2-layer where compared to the 1 ½-layer, and the very low peak density near midnight local time (far-right figure). In contrast to the equatorial profiles the comparison with the. 1'1 M model appears to be more favorable at the top-side than below the F2-peak.

In order to assess the accuracy of the GPS/MET retrievals, coincidences of other types of data such as ionosondes or incoherent scatter radar (ISR) with GPS/MET occultations have been searched for. To date, wc were able to find a single ISR measurement obtain from Millstone Hill which coincided with an occultation in space and time. Fig. 7 (top) shows a GPS/MET profile obtain on 1995-May-5, 0310 UT with tangent points coordinates around 42N and 282E. On the same figure is the ISR measurement of electron density obtained in the 320 microsecond pulse mode of operation and obtained 20 minutes after the occultation. On the bottom part of Fig. 7 is the same GPS/MET profile compared to several ISR profiles obtained around the time of the occultation with the ISR operating at the 640 microsecond pulse mode. Millstone Hill is located at 42.6N and 288.5E which is about 6" east of the occultation location. It is clear from Fig. 7 that the occultation retrieval best matches the ISR data collected at 034011'1'. The discrepancies between the ISR and the occultation can be ascribed to several factors, including the spatial anti temporal separation between the occultation and the ISR measurements, error introduced by the spherical symmetry assumption when doing the GPS/MET retrieval, anti error in the ISR measurements. It is clear that further comparisons to ground truth is needed for further assessment of the accuracy of the occultation retrievals.

Finally in this section wc examine some amplitude data obtained from GPS/MET. Fig. 8 shows the flight receiver signal-to-noise ratio of the L1 anti L2 signals for four different occultations where time = O corresponds to the start of high-rate at about 120 km altitude. The gradual decrease of SNR starting at about 30-40 seconds is due to significant atmospheric bending starting at about the tropopause. As the signal approaches the surface, it is significantly bent (up to - 1") anti defocused and finally disappears. Neal-ly half of the occultation displays a smooth steady SNR while the signal is in the ionosphere. Figure 8.d is an example of such smooth SNR. However, a good fraction of them (see Fig. 8a, b and c) show one or several sharp changes in SNR which can be attributed to sharp layers (e.g. sporadic E) at the. bottom of the ionosphere. That these scintillations are caused by the ionosphere and not the neutral atmosphere can be seen from the fact that the L2 SNR fluctuation is larger than that of L1, consistent with its lower carrier frequency.

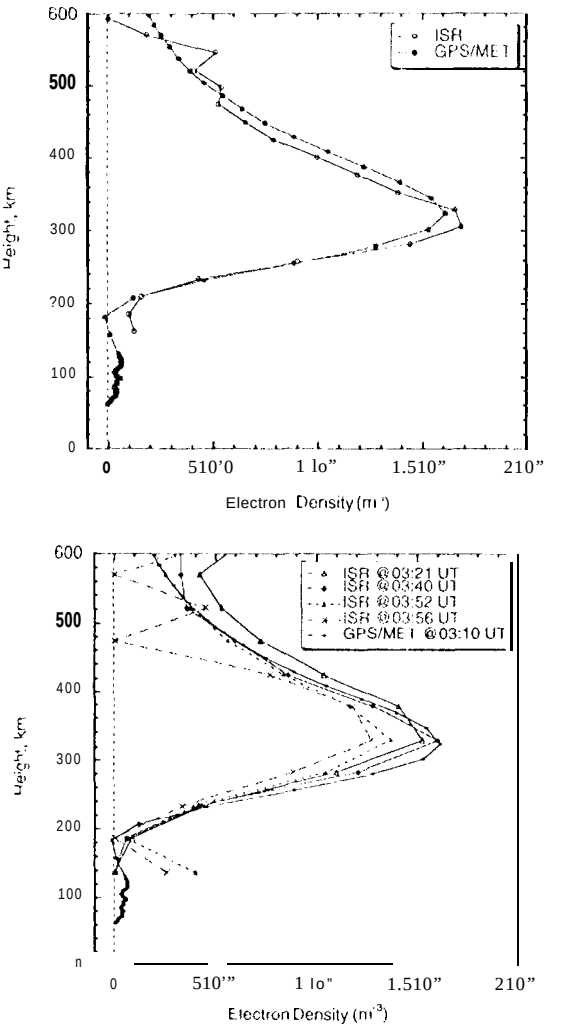

Fig. 7: Comparisons of electron density profile obtained from GPS/MET with coincident measurements from Millstone Hill ISR. Around the time of occultation the ISR operated in two modes, the 320 μsec pulse mode (top figure) and the 640 μsec pulse mode (bottom figure).

'1 'he electron density profiles obtained from the phase data via the Abel inversion corresponding to the occultations of Fig. 8 are shown in Fig. 9. Fig. 9a, b and c respectively show one, several anti two sharp layers at the bottom of the ionosphere. Another possible interpretation for some of these sharp scintillations is that they are caused by some structure in the F region missed due to sub-sampling of the occultation signal above 120 km (sample rate when tangent point > 120 km is 0.1Hz). A more careful examination of the 1,2 data and the time shift between these sharp scintillations for the L1 anti L2 signal should resolve some of the ambiguity as to where along the occulting link these ionospheric irregularities exist. This will be. performed in future work.

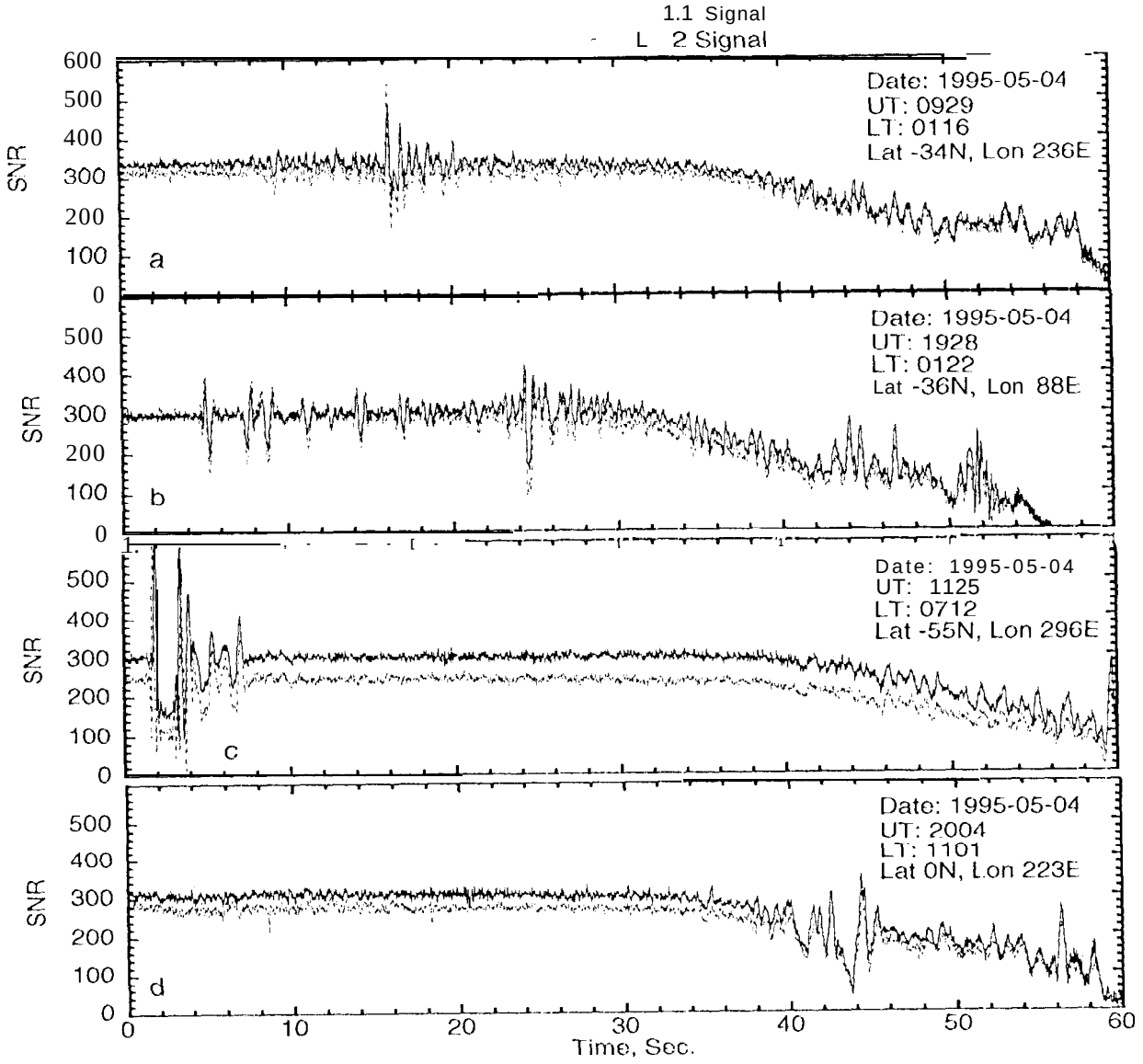

Fig. 8: Instrumental Sigr)a]-to-noise ratio as a function of time for L1 and L2 signals for four different occultations.

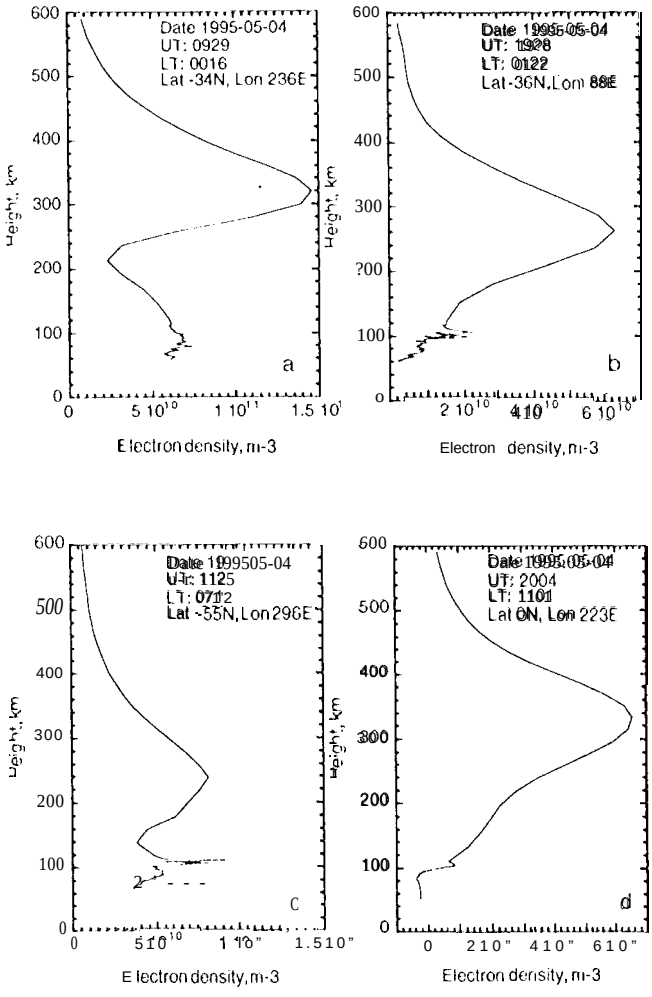

Fig. 9: GPS/MET profiles of electron density corresponding to occultations of Fig. 8.

ACKNOWLEDGMENTS

We thank M. Exner and R. Ware of UCAR for providing the GPS/MET flight data. We thank John Foster for providing the Millstone Hill ISR data. This research was performed at the Jet Propulsion Laboratory, California Institute of Technology, under the Director's Research Discretionary Fund.

REFERENCES

Ejeldbo G. E., V. R. Eshleman, A. J. Kliore, *Astron. J. -/6, 123,* 1971.

Hajj G. A., R. Ibanez-Meier, E. R. Kursinski, and L. J. Romans, "Imaging the Ionosphere with the Global Positioning System", *Int. J. of Imaging Sys. and Tech.*, Vol. 5, 174-184, 1994.

Hajj G. A., E. R. Kursinski, W. 1. Bertiger, S. S. Leroy, and J. T. Schofield, "Sensing the. Atmosphere, From a 1 ow-Earth Orbiter Tracking GPS: Early Results and Lessons From the GPS/MET Experiment", *Proc.* of ION-GPS 9 5, *The 8th International Technical Meeting of The Satellite Division of The Institute of Navigation*, pp *1167-1174, 1995.*

Kursinski E. R., G. A. Hajj, K. R. Hardy, L. J. Remans, and J. '1'. Schofield, *Geophy. Res. Lett.*, Vol. 22, No. 17, pp. 2365-2368, 1995.

Kursinski E. R, G. A. Hajj, W, 1. Bertiger, S. S, Leroy, T. K. Meehan, L. J. Romans, J. '1'. Schofield, D. J. McCleese, W. G. Melbourne, C. L. Thornton, 'I'. I'. Yunck, J. R. Eyre, and R. N. Nagatani, *Science*, Vol. 271, pp. 1107-1110, 1996a.

Kursinski E. R., G. A. Hajj, K. R. Hardy, J. '1'. Schofield, and R. Linfield, "Observing Earth's Atmosphere with Radio Occultation Measurements using GPS", submitted to *J. Geophys. Res.*, 1996b.

Leroy S., "The Measurement of Geopotential Heights by GPS Radio Occultation", submitted to *J. Geoph ys. Rev.*, **1996.**

Meehan et al, *6th Int. Geodetic Symp. on Satellite Positioning*, Columbus Ohio, 1992.

Tyler G. L., *Proc. IEEE*, 75: I 4041431, 1987.

Ware. R., M. Exner, D. Feng, M. Gorbunov, K. Hardy, B. Herman, Y. Kuo, T. Meehan, W. Melbourne, C. Rocken, W. Schreiner, S. Sokolovskiy, F. Solheim, X. Zou, R. Anthes, S. Businger, and K. Trenberth. "GPS sounding of the atmosphere from low earth orbit: preliminary results", *Bulletin of the American Meteorological Society,* Vol. 77, No. 1, pp. 19-40, 1996.